Ultrafast magnetization switching by spin-orbit torques

Kevin Garello,[1,a] Can Onur Avci,[1] Ioan Mihai Miron,[2,3,4] Manuel Baumgartner,[1] Abhijit Ghosh,[1] Stéphane Auffret,[2,3,4] Olivier Boulle,[2,3,4] Gilles Gaudin,[2,3,4] and Pietro Gambardella[1]

[1]Department of Materials, ETH Zürich, Hönggerbergring 64, Zürich CH-8093, Switzerland
[2]Université Grenoble Alpes, SPINTEC, 38000 Grenoble, France
[3]CEA, INAC-SPINTEC, 38000 Grenoble, France
[4]CNRS, SPINTEC, 38000 Grenoble, France

Spin-orbit torques induced by spin Hall and interfacial effects in heavy metal/ferromagnetic bilayers allow for a switching geometry based on in-plane current injection. Using this geometry, we demonstrate deterministic magnetization reversal by current pulses ranging from 180 ps to ms in Pt/Co/AlO$_x$ dots with lateral dimensions of 90 nm. We characterize the switching probability and critical current I_c as a function of pulse length, amplitude, and external field. Our data evidence two distinct regimes: a short-time intrinsic regime, where I_c scales linearly with the inverse of the pulse length, and a long-time thermally assisted regime, where I_c varies weakly. Both regimes are consistent with magnetization reversal proceeding by nucleation and fast propagation of domains. We find that I_c is a factor 3–4 smaller compared to a single domain model and that the incubation time is negligibly small, which is a hallmark feature of spin-orbit torques. © 2014 AIP Publishing LLC. [http://dx.doi.org/10.1063/1.4902443]

Magnetization switching is a topic of fundamental interest as well as of practical relevance for the development of fast, non-volatile data storage devices. In recent years, current-induced switching of nanosized magnets has emerged as one of the most promising technologies for the realization of a scalable magnetic random access memory (MRAM).[1] In the so-called spin transfer torque (STT)-MRAM, a spin-polarized current flowing through a pinned magnetic layer induces a torque on the storage layer that counteracts the magnetic damping.[2,3] STT switching can be made faster by increasing the injected current or choosing materials with low damping. However, when the magnetization of the reference and free layer are at rest, parallel or anti-parallel, the STT is zero. The resulting non-negligible incubation delay, governed by thermally activated oscillations, limits ultrafast switching and induces a broad switching time distribution.[4] Several solutions have been explored to reduce the incubation delay, such as biasing STT devices with a hard axis field[4] or adding an out-of-plane polarizer to an in-plane free layer.[5] This has led to switching times as low as 50 ps in metallic spin valves[6–8] and 500 ps in magnetic tunnel junctions (MTJ).[9] Despite such progress, the development of STT-MRAM for ultrafast applications such as cache memories remains problematic. Fast switching requires large current through the thin oxide barrier of a MTJ, which leads to reliability issues and accelerated aging of the barrier.

Spin-orbit torque (SOT)-induced switching, generated by the flow of an electrical current in the plane of a ferromagnetic/heavy metal (FM/HM) bilayer, offers an interesting alternative to STT.[10] Theoretical[11,12] and experimental[10,13–19] studies have evidenced significant antidamping $T^{\parallel} \propto m \times (y \times m)$ and field-like $T^{\perp} \propto m \times y$ SOT components in such systems, which originate from either the bulk spin

Hall effect in the HM layer or interfacial Rashba-type spin-orbit coupling, or a combination of these effects. $T^{\parallel}$ is responsible for the switching of the magnetization m. As this torque is directed parallel to y for a current directed along x, $T^{\parallel}$ destabilizes both directions of the magnetization and the application of a bias field along the current direction is required to stabilize one magnetic configuration over the other. Consequently, switching is bipolar with respect to both current and bias magnetic field.[10] SOT has proven very effective to switch the magnetization of perpendicular[10,20,21] and in-plane magnetized layers,[14,15] as well as to control the motion of domain walls in FM/HM heterostructures.[22–24] In
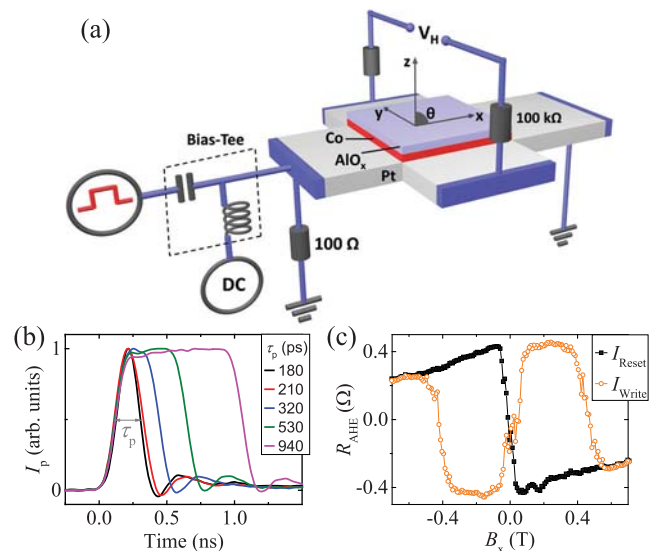

FIG. 1. (a) Schematic of the experimental setup. (b) Current pulses of different duration detected in transmission. (c) Magnetization switching of sample s1 induced by positive and negative current pulses with current density $I_p = 1.65$ mA and $\tau_p = 210$ ps, averaged over 100 pulses. B_x is swept only once from +0.65 to −0.65 T.

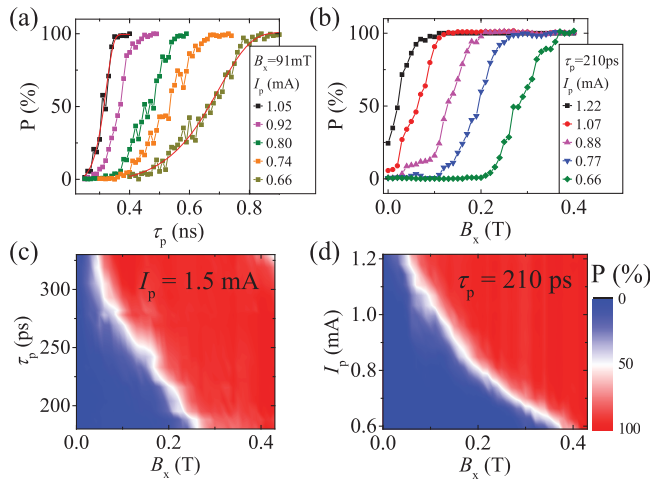a)Electronic mail: kevin.garello@mat.ethz.ch

FIG. 2. Switching probability of s1 as a function of (a) τ_p ($B_x = 91$ mT) and (b) B_x ($\tau_p = 210$ ps) at different current amplitudes. Two-dimensional diagrams of the switching probability showing successful (red) and unsuccessful (blue) events measured as a function of (c) τ_p and B_x for fixed $I_p = 1.5$ mA and (d) I_p and B_x for fixed $\tau_p = 210$ ps.

SOT devices with perpendicular magnetic anisotropy (PMA), as $T^{\parallel}$ is always perpendicular to the magnetization, the incubation delay of the switching process is expected to be minimum. Moreover, SOT allows for the separation of the read and write current paths in an MTJ, avoiding electrical stress of the tunnel barrier during writing. Based on these considerations, novel SOT-MRAM architectures have been proposed[25,26] and the switching of in-plane[14,15,27] and out-of-plane MTJ has been recently demonstrated.[28] There is, however, no systematic study of SOT switching on a sub-ns timescale. In this letter, we investigate the probability of SOT-induced magnetization reversal of perpendicularly magnetized Pt/Co/AlO$_x$ dots as a function of current pulse width, amplitude, and external magnetic field on timescales ranging from 180 ps to ms.

Pt(3 nm)/Co(0.6 nm)/AlO$_x$ layers with PMA were deposited by magnetron sputtering and patterned into square dots on top of Pt Hall bars, as described in Ref. 10. We present results for three different samples of lateral size s1 = 90 nm, s2 = 95 nm, and s3 = 102 nm, as measured by scanning electron microscopy. These samples have a saturation magnetization $M_s \approx 8.7 \times 10^5$ A/m (measured before patterning) and an effective anisotropy field $B_k \approx 2K/M_s - \mu_0 M_s \approx 1$ T. Figure 1(a) shows a schematic of the measurement setup. In order to ensure the transmission of fast pulses without significant reflection due to the large resistance of the Pt contacts (~2 kΩ), a 100 Ω resistor is connected in parallel with the sample. A 100 kΩ series resistor prevents spreading of the current pulses into the Hall voltage probes. An in-plane bias magnetic field (B_x), determining the switching polarity for a given current polarity,[10] is applied along the current line, with a tilt of 0.5° towards z in order to favor a homogeneous magnetization when no current pulses are applied. The perpendicular component of the magnetization is measured via the anomalous Hall resistance ($R_{AHE} = 0.45$ Ω at saturation) using a low DC current of 20 µA. A bias tee separates the current pulses and the DC current. All measurements are performed at room temperature. To study the

switching probability distribution, we proceed as follows: first, a positive 0.7 mA "reset" pulse of 20 ns duration is used to initialize the magnetization direction. Second, a negative "write" pulse of length τ_p and amplitude I_p is applied. R_{AHE} is measured a few milliseconds after each pulse. The switching probability is defined as $P = [R_{AHE}^{write}(I_p, \tau_p, B_x) - R_{AHE}^{reset}(B_x)] / \Delta R_{AHE}(B_x)$ averaged over 100 trials. $\Delta R_{AHE}(B_x)$ is the difference between the Hall resistance of the up and down states measured during a sweep of B_x at the same field at which the switching is performed. Switching diagrams are constructed by varying two out of the three free parameters τ_p, I_p, and B_x while the other one is kept constant.

Figure 1(c) shows the magnetic state of sample s1 after applying write pulses with $\tau_p = 210$ ps and $I_p = 1.65$ mA (open orange circles) as a function of B_x. The magnetization after the reset operation is shown as solid black squares. B_x is swept in steps from −0.65 to 0.65 T. At each field step, R_{AHE} is determined as described above. Switching can be experimentally observed in the hysteretic range delimited by the coercive field of the Co layer ($B_c \approx 0.45$ T). The orange and black curves indicate that for $B_x > 0$ a current $I_p > 0$ switches the magnetization downwards and $I_p < 0$ switches it upwards, whereas for $B_x < 0$ the effect of the current polarity is reversed. This behavior is typical of SOT and similar to that reported for single pulses ranging from tens of ns to µs in devices with size varying from 200 to 1000 nm.[10,20,21,28]

Since switching occurs on such short timescales and considering the analogy between orthogonal-STT devices and SOT (polarization of the spin current perpendicular to the magnetization), effects related to the magnetization precession are expected to be important when varying τ_p and I_p.[7,29] Moreover, macrospin simulations show that $T^{\perp}$ (equivalent to an effective field along y) promotes oscillations of the magnetization with periods up to ns, thus inducing precessional switching even for high damping constants such as $\alpha = 0.5$. We therefore measured the switching probability as a function of τ_p and I_p, as well as of B_x, which, besides being necessary for switching, influences the SOT-induced dynamics. Figures 2(a) and 2(b) show representative measurements of P as a function of τ_p and B_x, respectively, for different values of I_p. By repeating such measurements over a grid of (B_x, τ_p) and (B_x, I_p) pairs, we construct the switching diagrams reported in Figures 2(c) and 2(d). The red (blue) color represents high (low) switching probability. In both diagrams, the range of successful switching events grows monotonically as either I_p, τ_p or B_x increase. We observe that the white boundary region representing intermediate P values is relatively narrow. Moreover, we do not observe oscillations of P beyond this boundary as a function of I_p or τ_p, as would be expected for precessional switching.[7,29] In fact, SOT-induced magnetization reversal in our samples is deterministic and bipolar with respect to either field or current down to $\tau_p = 180$ ps.

I_p and τ_p determine the energy dissipation during the switching process and the speed at which this can be achieved for a given bias field. Figure 3 shows the critical switching current I_c, defined at $P = 90\%$, as a function of τ_p measured over eight orders of magnitude in pulse duration for $B_x = 91$ mT. We find that there are two very different regimes: at short-time scales ($\tau_p < 1$ ns), I_c increases strongly
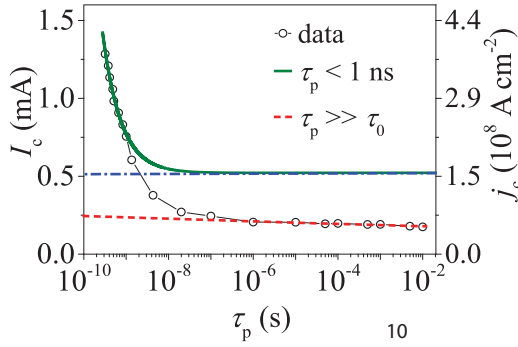
FIG. 3. Critical switching current of sample s2 as a function of pulse duration measured with $B_x = 91$ mT. The green solid line is a fit to the data in the short-time regime ($\tau_p < 1$ ns) according to Eq. (1). The red dashed line is a fit to the data in the thermally activated regime ($\tau_p \geq 1 \mu$s) according to Eq. (2). The blue dash-dotted line represents the intrinsic critical current I_{c0}.

when reducing τ_p, whereas on longer time scales ($\tau_p \geq 1 \mu$s), I_c has a weak dependence on τ_p. This behavior is qualitatively similar to that observed in STT devices[30–32] and associated with an intrinsic regime where the switching speed depends on the efficiency of angular momentum transfer from the current to the magnetic layer and a thermally assisted regime in which stochastic fluctuations help the magnetization to overcome the reversal energy barrier.

We focus first on the short-time regime. In this limit, I_c is inversely proportional to τ_p, as shown in Figure 4. Similar behavior is observed for samples s1–s3, indicating that the τ_p^{-1} dependence is specific to the switching process rather than to a particular sample. In analogy with STT,[31,32] we model I_c as

$$I_c = I_{c0} + \frac{q}{\tau_p}, \tag{1}$$

where I_{c0} is the intrinsic critical switching current and q is an effective charge parameter that represents the number of electrons that needs to be pumped into the system before reversal occurs, describing the efficiency of angular momentum transfer from the current to the spin system. From the fit shown in Fig. 4, we obtain $I_{c0} = 0.58$ mA ($j_{c0} = 1.76 \times 10^8$ Acm^{-2}) and $q = 2.1 \times 10^{-13}$ C. This linear relationship holds for different B_x [Fig. 4]. When increasing B_x from 91 to 146 mT, q decreases by about 13%, whereas I_{c0}
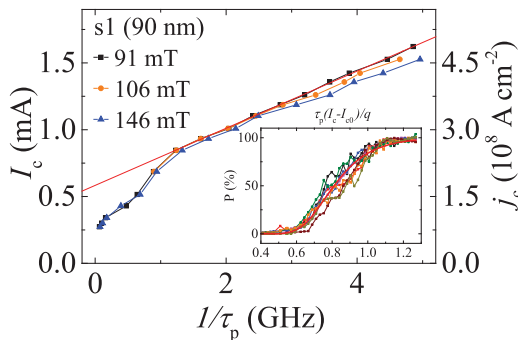

FIG. 4. Critical switching current of sample s1 as a function of $1/\tau_p$ for different values of B_x. The thin red line shows a linear fit to the short-time data ($1/\tau_p > 1$ GHz) measured at $B_x = 91$ mT using Eq. (1). Inset: P in the short-time regime as a function of $\tau_p (I_c - I_{c0})/q$. The red line represents an average fit of all the curves using a sigmoidal function.

increases from 0.58 to 0.61 mA. Further proof that the linear dependence of I_c on τ_p^{-1} is general to the switching distribution and not dependent on the definition of the critical current is reported in the inset of Fig. 4, showing that all the switching probability curves measured for $\tau_p < 1$ ns, plotted as a function of the scaled angular momentum $(I_c - I_{c0})\tau_p / q$, fall onto the same curve.

The experimental I_{c0} can be compared with that expected from monodomain SOT-induced magnetization reversal,[33] given by the condition $T^{\parallel}(I_{c0}) = (B_k/2 - B_x/\sqrt{2})$. This torque is often expressed in terms of an effective spin Hall angle θ_{SH}^{eff} as $T^{\parallel} = [\hbar/(2e)\theta_{SH}^{eff}/(M_s t_{FM})]j$, where t_{FM} is the thickness of the FM layer and the current density j is assumed to be uniform throughout the FM/HM bilayer,[33,34] which is a reasonable assumption for Co/Pt. θ_{SH}^{eff} is a useful parameter to compare results from different experiments, but does not correspond to the bulk spin Hall angle of the HM layer, as it takes into account neither the finite spin diffusion length in the HM nor FM/HM interface effects. Here, by considering the ratio $T^{\parallel}/j = 6.9$ mT/10^7 Acm^{-2} ($\theta_{SH}^{eff} = 0.11$) obtained from harmonic Hall voltage measurements of Pt(3 nm)/Co(0.6)/AlO$_x$ dots in the quasistatic, low current ($j \leq 10^7$ Acm^{-2}) limit,[16] we estimate $I_{c0} \approx 2.05$ mA. This value is about 3.5 times larger compared to the experiment. In order to match the critical current of our samples to the macrospin prediction, θ_{SH}^{eff} should be about 0.4, an unreasonably large value for Pt.[35] As τ_p is too fast for thermally assisted switching, this comparison suggests that the magnetization reverses by a more current-efficient process than coherent rotation of a single magnetic domain.

Further support for this hypothesis comes from macrospin simulations of SOT switching in the sub-ns regime using the Landau-Lifshitz-Gilbert equation (not shown), which reveals that $I_c \sim \tau_p^{-\beta}$ with $\beta \approx 2$ rather than $\beta = 1$ as found in the experiment. This behavior differs from the macrospin dynamics of perpendicular magnetic layers induced by STT, for which our simulations confirm the linear scaling ($\beta = 1$) found in Ref. 32. The difference between SOT and STT stems from the competition between $T^{\parallel}$ and the anisotropy torque, which tend to align the magnetization, respectively, along y and z, whereas in the STT case, they both tend to align it towards z.

The inconsistency between macrospin models and our experiment suggests that magnetization reversal occurs by domain nucleation and propagation. In such a scenario, once a reverse domain nucleates due to the $T^{\parallel}$ and $T^{\perp}$, switching is achieved by the propagation of a domain wall through the dot. Since the domain wall velocity is proportional to j, the critical switching current is expected to be proportional to τ_p^{-1}, in agreement with our results in the short-time regime and Eq. (1). In this case, the "effective charge" q is inversely proportional to the domain wall velocity and can be interpreted as the angular momentum required to switch the entire dot once the reversal barrier of a portion of the sample has been overcome. The ratio between domain wall velocity and current density can be estimated by taking the width w of the sample as the distance that a domain wall has to travel before switching occurs and divide it by the time τ required to cover this distance. This time can be estimated as $\tau = q/jS$, so that $v/j = wS/q = 137$ (m/s)/10^8 Acm^{-2}, where $S = w(t_{FM} + t_{HM})$

is the cross section of the FM/HM bilayer. This ratio increases with the increase in B_x, as would domain wall speed, and is in quite good agreement with the large current-induced domain wall velocities (100–400 m/s) reported on similar structures.[22,23] We further note that micromagnetic simulations studies of FM/HM bilayers with large spin-orbit interaction proposed similar magnetization reversal scenarios,[36–39] pointing out also the important role played by the chirality of the walls.[22–24,39]

In the thermally assisted region ($\tau_p \gg 1$ ns), I_c is predicted to be[34]

$$I_c = \frac{B_k}{4}\frac{j}{T^{\parallel}}S\left(\pi - 2b_x - \sqrt{\frac{8}{\xi}\ln\left(\frac{-\tau_p}{\tau_0\ln(1-P)}\right)} \atop -8 - 4b_x^2 - 4b_x(\pi-4) + \pi^2\right), \tag{2}$$

where $\xi = B_k M_s w^2 t_{FM}/2k_B T$ is the thermal stability factor, $b_x = B_x/B_k$, and τ_0 the thermal attempt time. Although this expression is derived analytically in the framework of a macrospin model, we find that it fits reasonably well to our data (dashed line in Fig. 3). The fit, performed for τ_p between 1 μs and 10 ms by taking $\tau_0 = 1$ ns (estimated from the inflection point of the curve in Fig. 4), $b_x = 0.091$, and $P = 0.9$, gives $\xi = 110$. As for sample s3 $\xi \approx 700$ at room temperature, the smaller value of ξ derived from the fit indicates that the Co layer is not reversing as a monodomain, in agreement with the conclusions drawn from the short-time regime and similar to perpendicularly magnetized nanopillars.[31,40] An important result from this analysis is that the intercept of the fit in the thermally assisted region (dashed line in Fig. 3) and the intrinsic current determined in the short-time regime (dash-dotted line) gives the incubation time of the switching process,[31,32] which we find to be negligibly small ($\sim 10^{-20\pm2}$ s). Due to the weak dependence of I_c on τ_p in the thermally assisted regime, this result is largely independent of the function used to fit the data.

In conclusion, we have demonstrated non-stochastic bipolar switching of 90 nm magnetic dots induced by SOT using in-plane injection of current pulses down to 180 ps, and we confirm that the incubation time is negligibly small. This makes SOT-based heterostructures a promising candidate for ultra-fast recording applications such as MRAMs and cache memories. Similar to STT, we find that the dependence of the critical switching current on the pulse length can be divided into a short-time (intrinsic) regime and a long-time (thermally assisted) regime. For $\tau_p < 1$ ns, the critical switching current is inversely proportional to τ_p, contrary to the precessional behavior expected of a single domain magnet and consistent with a scenario where the switching speed is determined by domain wall propagation. In the single domain limit, the ratio between the SOT and STT critical current scales as[33] $I_{c0}^{SOT}/I_{c0}^{STT} = \frac{1}{2\alpha}\frac{\eta}{\theta_{SH}^{eff}}\frac{t_{FM}+t_{HM}}{w}$, where a large spin polarization η and low damping α favor STT, whereas a large θ_{SH}^{eff} and the smaller cross section of the current injection line favor SOT. Our results indicate that ultrafast SOT switching may compare more favorably to STT when domain propagation is involved.

[1] J. Hutchby and M. Garner, *IRTS Report on Emerging Memory Devices* (www.irts.net, 2010).
[2] J. C. Slonczewski, J. Magn. Magn. Mater. **159**, L1 (1996).
[3] B. Dieny, R. Sousa, J. Herault, C. Papusoi, G. Prenat, U. Ebels, D. Houssameddine, B. Rodmacq, S. Auffret, L. Buda-Prejbeanu *et al.*, Int. J. Nanotechnol. **7**, 591 (2010).
[4] T. Devolder, C. Chappert, J. Katine, M. Carey, and K. Ito, Phys. Rev. B **75**, 064402 (2007).
[5] A. Kent, B. Özyilmaz, and E. Del Barco, Appl. Phys. Lett. **84**, 3897 (2004).
[6] A. Tulapurkar, T. Devolder, K. Yagami, P. Crozat, C. Chappert, A. Fukushima, and Y. Suzuki, Appl. Phys. Lett. **85**, 5358 (2004).
[7] C. Papusoi, B. Delaët, B. Rodmacq, D. Houssameddine, J. Michel, U. Ebels, R. Sousa, L. Buda-Prejbeanu, and B. Dieny, Appl. Phys. Lett. **95**, 072506 (2009).
[8] O. J. Lee, D. C. Ralph, and R. A. Buhrman, Appl. Phys. Lett. **99**, 102507 (2011).
[9] H. Liu, D. Bedau, D. Backes, J. Katine, J. Langer, and A. Kent, Appl. Phys. Lett. **97**, 242510 (2010).
[10] I. M. Miron, K. Garello, G. Gaudin, P.-J. Zermatten, M. V. Costache, S. Auffret, S. Bandiera, B. Rodmacq, A. Schuhl, and P. Gambardella, Nature **476**, 189 (2011).
[11] P. M. Haney, H.-W. Lee, K.-J. Lee, A. Manchon, and M. Stiles, Phys. Rev. B **87**, 174411 (2013).
[12] X. Wang and A. Manchon, Phys. Rev. Lett. **108**, 117201 (2012).
[13] I. M. Miron, G. Gaudin, S. Auffret, B. Rodmacq, A. Schuhl, S. Pizzini, J. Vogel, and P. Gambardella, Nat. Mater. **9**, 230 (2010).
[14] L. Liu, C.-F. Pai, Y. Li, H. Tseng, D. Ralph, and R. Buhrman, Science **336**, 555 (2012).
[15] C.-F. Pai, L. Liu, Y. Li, H. Tseng, D. Ralph, and R. Buhrman, Appl. Phys. Lett. **101**, 122404 (2012).
[16] K. Garello, I. M. Miron, C. O. Avci, F. Freimuth, Y. Mokrousov, S. Blügel, S. Auffret, O. Boulle, G. Gaudin, and P. Gambardella, Nat. Nanotechnol. **8**, 587 (2013).
[17] J. Kim, J. Sinha, M. Hayashi, M. Yamanouchi, S. Fukami, T. Suzuki, S. Mitani, and H. Ohno, Nat. Mater. **12**, 240 (2013).
[18] X. Fan, H. Celik, J. Wu, C. Ni, K.-J. Lee, V. O. Lorenz, and J. Q. Xiao, Nat. Commun. **5**, 3042 (2014).
[19] T. D. Skinner, M. Wang, A. T. Hindmarch, A. W. Rushforth, A. C. Irvine, D. Heiss, H. Kurebayashi, and A. J. Ferguson, Appl. Phys. Lett. **104**, 062401 (2014).
[20] C. O. Avci, K. Garello, I. M. Miron, G. Gaudin, S. Auffret, O. Boulle, and P. Gambardella, Appl. Phys. Lett. **100**, 212404 (2012).
[21] C. O. Avci, K. Garello, C. Nistor, S. Godey, B. Ballesteros, A. Mugarza, A. Barla, M. Valvidares, E. Pellegrin, A. Ghosh, I. M. Miron, O. Boulle, S. Auffret, G. Gaudin, and P. Gambardella, Phys. Rev. B **89**, 214419 (2014).
[22] I. M. Miron, T. Moore, H. Szambolics, L. D. Buda-Prejbeanu, S. Auffret, B. Rodmacq, S. Pizzini, J. Vogel, M. Bonfim, A. Schuhl *et al.*, Nat. Mater. **10**, 419 (2011).
[23] S. Emori, U. Bauer, S.-M. Ahn, E. Martinez, and G. S. Beach, Nat. Mater. **12**, 611 (2013).
[24] K.-S. Ryu, L. Thomas, S.-H. Yang, and S. Parkin, Nat. Nanotechnol. **8**, 527 (2013).
[25] G. Gaudin, I. Miron, P. Gambardella, and A. Schuhl, WO 2012/014131A1, 2012/014132A1, 2012/056348A1 (2012).
[26] A. van den Brink, S. Cosemans, S. Cornelissen, M. Manfrini, A. Vaysset, W. Van Roy, T. Min, H. Swagten, and B. Koopmans, Appl. Phys. Lett. **104**, 012403 (2014).
[27] M. Yamanouchi, L. Chen, J. Kim, M. Hayashi, H. Sato, S. Fukami, S. Ikeda, F. Matsukura, and H. Ohno, Appl. Phys. Lett. **102**, 212408 (2013).
[28] M. Cubukcu, O. Boulle, M. Drouard, K. Garello, C. O. Avci, I. M. Miron, J. Langer, B. Ocker, P. Gambardella, and G. Gaudin, Appl. Phys. Lett. **104**, 042406 (2014).

[29]M. M. de Castro, R. Sousa, S. Bandiera, C. Ducruet, A. Chavent, S. Auffret, C. Papusoi, I. Prejbeanu, C. Portemont, L. Vila *et al.*, J. Appl. Phys. **111**, 07C912 (2012).

[30]R. Koch, J. Katine, and J. Sun, Phys. Rev. Lett. **92**, 088302 (2004).

[31]D. Bedau, H. Liu, J. Sun, J. Katine, E. Fullerton, S. Mangin, and A. Kent, Appl. Phys. Lett. **97**, 262502 (2010).

[32]H. Liu, D. Bedau, J. Sun, S. Mangin, E. Fullerton, J. Katine, and A. Kent, J. Magn. Magn. Mater. **358**, 233 (2014).

[33]K.-S. Lee, S.-W. Lee, B.-C. Min, and K.-J. Lee, Appl. Phys. Lett. **102**, 112410 (2013).

[34]K.-S. Lee, S.-W. Lee, B.-C. Min, and K.-J. Lee, Appl. Phys. Lett. **104**, 072413 (2014).

[35]A. Hoffmann, IEEE Trans. Magn. **49**, 5172 (2013).

[36]G. Finocchio, M. Carpentieri, E. Martinez, and B. Azzerboni, Appl. Phys. Lett. **102**, 212410 (2013).

[37]E. Martinez, S. Emori, and G. S. Beach, Appl. Phys. Lett. **103**, 072406 (2013).

[38]N. Perez, E. Martinez, L. Torres, S.-H. Woo, S. Emori, and G. Beach, Appl. Phys. Lett. **104**, 092403 (2014).

[39]O. Lee, L. Liu, C. Pai, Y. Li, H. Tseng, P. Gowtham, J. Park, D. Ralph, and R. Buhrman, Phys. Rev. B **89**, 024418 (2014).

[40]D. P. Bernstein, B. Bräuer, R. Kukreja, J. Stöhr, T. Hauet, J. Cucchiara, S. Mangin, J. A. Katine, T. Tyliszczak, K. W. Chou *et al.*, Phys. Rev. B **83**, 180410 (2011).